PERGAMON

International Journal of Multiphase Flow 26 (2000) 1235–1246

International Journal of Multiphase Flow

www.elsevier.com/locate/ijmulflow

Heat transfer in horizontal solid–liquid pipe flow

R. Rozenblit [a], M. Simkhis [b], G. Hetsroni [a,*], D. Barnea [b], Y. Taitel [b]

[a] *Department of Mechanical Engineering, Technion-Israel Institute of Technology, Haifa, Israel*
[b] *Department of Fluid Mechanics and Heat Transfer, Faculty of Engineering, Tel Aviv University, Tel Aviv, Israel*

Received 15 February 1999; received in revised form 19 July 1999

Abstract

An experimental study of the heat transfer coefficient associated with solid–liquid mixture transport was carried out using an electro-resistance sensor and infra-red imaging. The average heat transfer increases with particle concentration. The local value of the heat transfer coefficient is strongly influenced by the cross sectional distribution of the solid phase in the pipe. At flow regimes associated with low mixture flow rates and substantial settled bed, the heat transfer at the bed periphery deteriorates because of the ''screen effect'' produced by the settled particles. In some cases, this phenomenon may cause local overheating. The analysis of the near wall structures, obtained from the temperature field, has shown that at a relatively high velocity where the bed is thin and flat the streaky structure is close to the one observed in a single phase flow, while at low mixture velocities, where the bed is thick and well packed the typical streaky structures of clear water are destroyed. It is shown that the modified Boltzman function fits the concentration profiles for the case of a moving bed regime. Good agreement is found between the bed height, obtained from experimental data, and the one predicted by the three-layer model.

Keywords: Slurry flow; Heat transfer; Concentration distribution; Particle-laden flow; Turbulence structure

1. Introduction

Slurry transportation from reactors to places where materials are utilized or stored is strongly influenced by the heat exchange between the transported materials and the surrounding. The heat transfer in slurry pipelines is affected by the cross sectional solid phase

* Corresponding author.

0301-9322/00/$ - see front matter
PII: S0301-9322(99)00089-0

distribution. Since the slurry reactor design requires characteristics of the heat removal to be known, the heat transfer from the slurry to the heated wall is a subject of intense interest.

Various flow patterns can be encountered in solid–liquid pipelines that affect the hydrodynamics of the flow and the mechanism of heat transfer. The slurry flow behavior depends strongly on the mixture flow rate and the delivery concentration of the particles. The solid–liquid flow patterns are classified according to the solid phase distribution in the carrier liquid. The main flow patterns observed in slurries of coarse particles are: stationary bed, moving bed, heterogeneous flow, and pseudo-homogeneous flow patterns. (Doron and Barnea, 1996; Shook and Roco, 1991; Televantos et al., 1979; Wilson et al., 1972). Under certain conditions the bed takes a form of "dunes" like periodic flow (Thomas, 1964).

Slurry flow structure can be assessed from concentration distribution measurements as demonstrated by Nasr-el-din et al. (1987). A non-intrusive electro-resistance sensor for concentration measurements in narrow pump channels was proposed by Creutz and Mewes (1999). Ozbelge and Somer (1988) measured both cross sectional solid phase distribution and bulk heat transfer coefficient in horizontal solid–liquid suspension flow.

Analytical prediction of concentration profiles in solid-liquid flow is reported by Taylor (1954) and Foster et al. (1992). The three-layer model presented by Doron and Barnea (1993) for flow pattern and pressure drop predictions yields also the concentration distribution in the pipe cross section.

The effect of solid particles on the heat transfer in turbulent flow has been the subject of many experimental investigations. Wilkinson and Norman (1967), and Hasegawa et al. (1983) studied this effect in solid–gas flow, while Harada et al. (1985, 1989), Agarwal (1988) and Hetsroni and Rozenblit (1994) in solid–liquid mixtures. Quader and Wilkinson (1981) discussed the limitations of using the analogy between heat and momentum transfer.

The heat transfer coefficient is usually correlated by using a modification of the Sieder–Tate equation or other empirical formulas. No attention was paid to the local heat transfer modification due to the particles. Significant attention, on the other hand, was paid to the effect of the solid particles on the turbulence and coherent structure in the vicinity of the wall, which play a dominant part in the heat transfer mechanism. The alternating streaks of high and low speed fluid, associated with the velocity field near the wall were observed. The streaks do not exhibit steady behavior or uniform distribution. Nevertheless, it is possible to estimate a mean spanwise spacing of streaks. The large particles do not follow the streaky structure whereas small ones, generally are accumulated along the low speed streaks, as was found by Hetsroni and Rozenblit (1994) by means of their infrared technique and by Kaftori et al. (1995). Nino and Garsia (1996) reported that the velocity of large particles corresponds to the streaky structure.

The main objectives of the present study are to estimate the influence of slurry flow on the local heat transfer coefficient, and describe the turbulent coherent structure evolution induced by the particles. In the present work the moving bed pattern is considered. The interface of the moving bed is either wavy (dune regime) at low velocities or flat (flat bed regime) at high mixture flow rates.

In order to observe the particle influence on the heat transfer in solid liquid mixture flow, the local heat transfer coefficient is measured using the IR image technique combined with chord concentration measurements.

The solid–liquid mixture is composed of plastic acetal particles suspended in clear water and flowing as a mixture in a horizontal pipe. The experimental results include the temperature distribution on the heated wall and the vertical chord concentration distribution. The data are used to calculate the local as well as the average values of the heat transfer coefficients. The near wall structures available from the temperature field in single phase flow is compared to those associated with different slurry flow patterns. A simultaneous qualitative analysis of the near wall structures and the corresponding solid phase concentration profiles is performed.

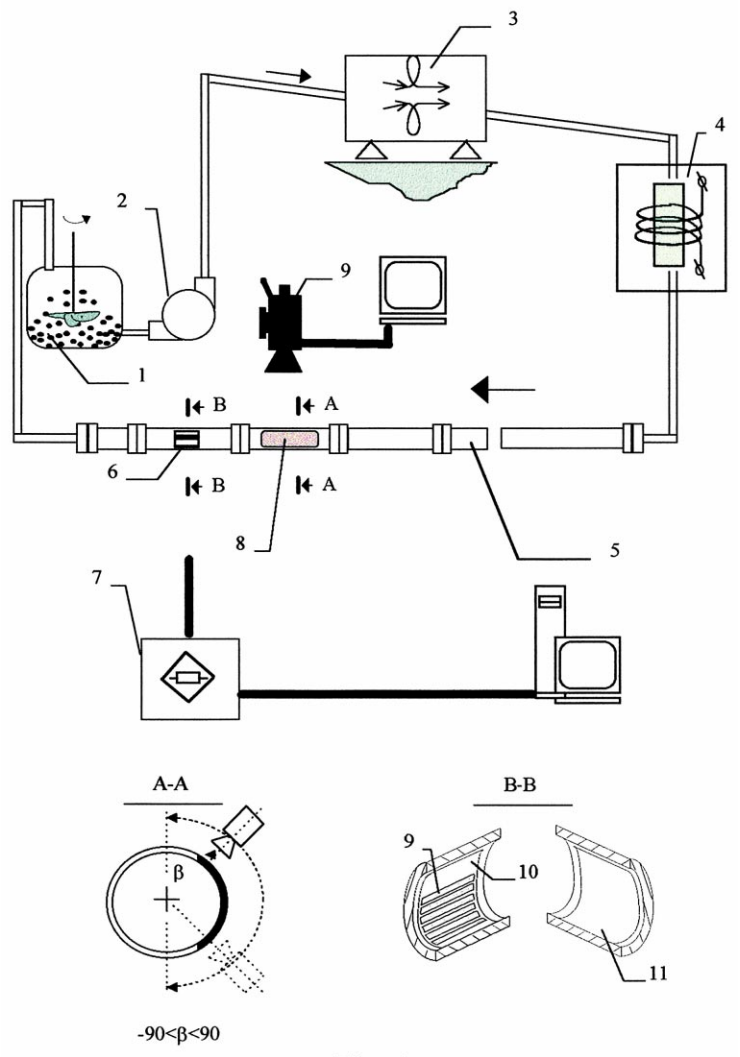

Fig. 1. Experimental system.

2. Experimental

The experimental facility is given schematically in Fig. 1. It includes a slurry tank (1) fitted with a variable speed mixer, a variable speed slurry pump (2), a mass flow meter (3) for simultaneous measurements of the mixture flow rate and mixture density; a magnetic flow meter (4) for volumetric flow rate measurements and a 10 m long test section made of a transparent pipe (5) which allows visual observation of the slurry flow patterns.

The solid–liquid mixture contains spherical shape coarse particles with a density of 1240 kg/m^3 and a diameter of 3.0 mm, suspended in clear water.

A special tomographic sensor (6) and a control unit (7) are used for chord concentration measurements and an infrared camera is used to measure the heat transfer characteristics.

The sensor operational principle is based on the dependence of the mixture conductivity on the concentration of non-conducting particles suspended in a conducting liquid (Creutz and Mewes, 1999; Simkhis et al., 1998).

The sensor cross section is shown schematically in Fig. 1. The sensor consists of an array of 16 strip electrodes (9) pasted on one half of the periphery, a shield electrode (10) and a common electrode (11) placed on the other half. An electronic multiplexer provides sequential measurements of the resistance between any electrode and the common one which yields the resistance of the mixture at a certain level. Calibration of the resistance allows to translate these readings into local concentrations. This sensor is designed to take a continuous reading of the local concentration at all levels of the pipe cross section.

The pipe wall temperature was measured using a setup which consists of a heating section (8) and an IR camera (9) attached to a video recording system and a PC. The heating section is constructed as a window of 50 μm thick Constantan foil attached to the inner plastic tube wall and heated by d.c. current.

The angular dimension of the window was 70°. In order to measure the time average foil temperature corresponding to different angular coordinates this section was rotated so that the

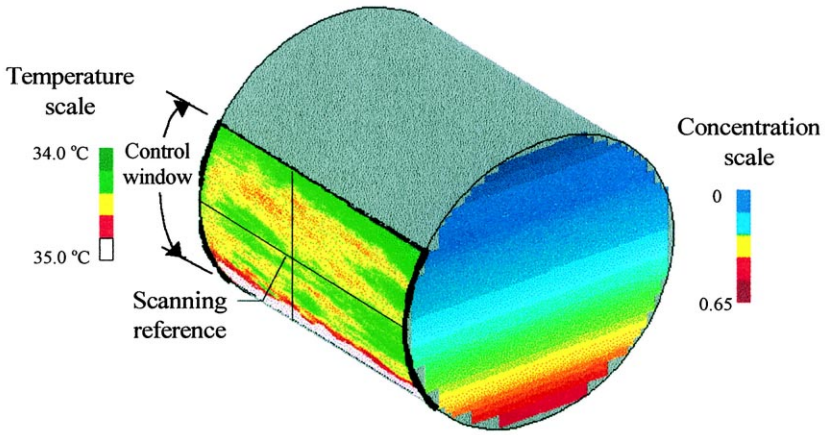

Fig. 2. Illustration of the temperature measurement.

measurements cover the range from -90° to 90°, as shown in the cross section view A–A in Fig. 1.

Two liquid Reynolds numbers were used. The first one ($Re_w = 19\ 000$) is within the dune regime while the second one ($Re_w = 55\ 000$) is in the flat moving bed regime (Fig. 2). The tested volumetric concentrations were 6%, 9%, 12%, and 15%.

The local temperatures have been averaged over a time interval of several minutes. The local time average heat transfer coefficient is:

$$\alpha = \frac{q}{(t_s - t_\infty)} \tag{1}$$

where q is the input heat flux; t_s, the local time average wall temperature; t_∞, the slurry flow bulk temperature.

The dimensionless heat transfer coefficient is defined as follows:

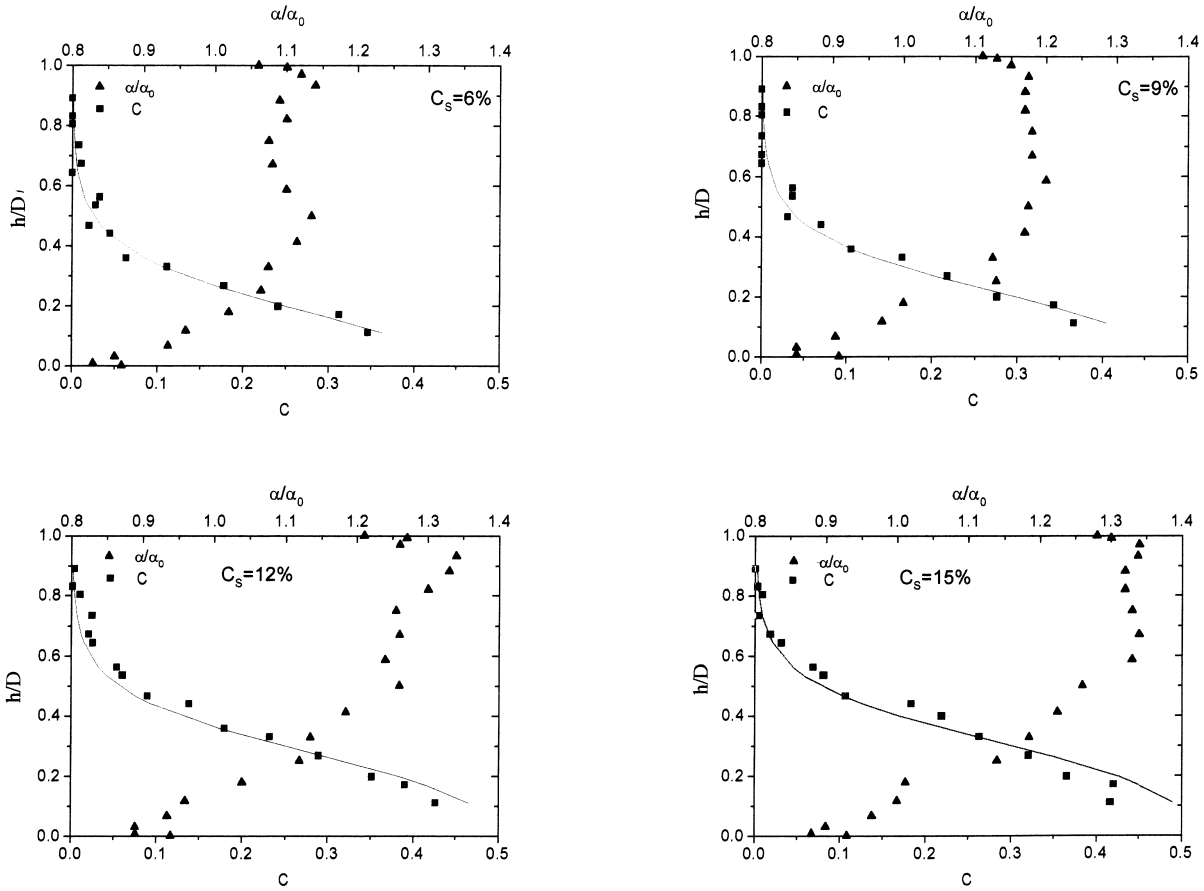

Fig. 3. Concentration and heat transfer coefficient profiles for the flat moving bed regime ($Re_w = 55\ 000$).

$$\tilde{\alpha} = \frac{\alpha}{\alpha_0} \tag{2}$$

where: α_0 is the heat transfer coefficient in clear liquid.

The cross sectional average heat transfer coefficient is:

$$\bar{\alpha} = \frac{Q}{A(\bar{t}_s - t_\infty)} \tag{3}$$

where

$$\bar{t}_s = \frac{1}{\pi D}\int_0^{2\pi} t_s \frac{D}{2} \mathrm{d}\beta \tag{4}$$

and D is the pipe diameter.

More on the infrared measurement technique is detailed in Hetsroni et al. (1998). The chord concentration profiles are determined as an average of at least 300 consequent profiles obtained

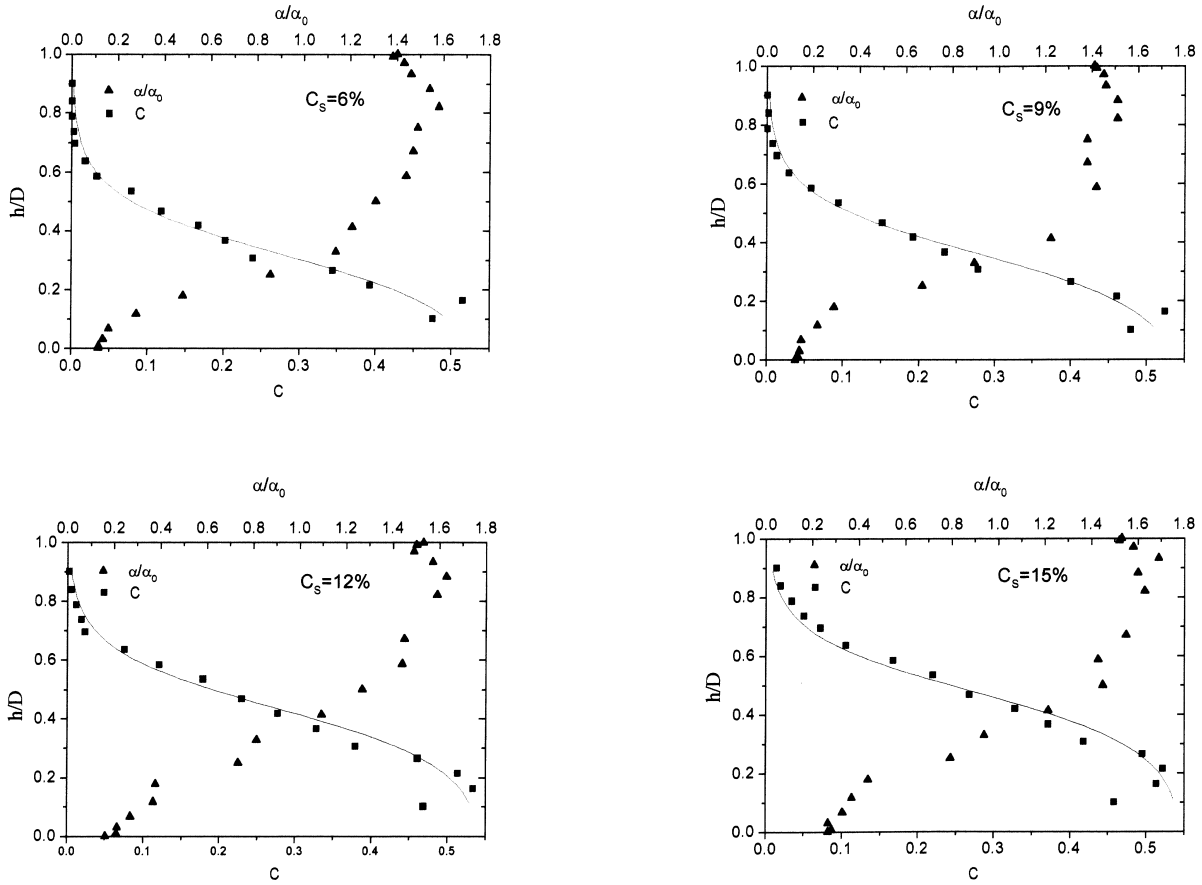

Fig. 4. Concentration and heat transfer coefficient profiles for the dune regime ($Re_w = 19\,000$).

by using an electro-resistance sensor. Details on this technique can be found in Simkhis et al. (1998).

3. Experimental results

Combined concentration and heat transfer coefficient profiles for the flat moving bed regime ($Re_w = 55\ 000$) and the dune regime ($Re_w = 19\ 000$) are shown in Figs. 3 and 4, respectively. $\bar{h} = h/D$ is the dimensionless level above the bottom of the pipe (D is the pipe diameter). As can be seen from the graphs, the concentration profiles show an exponential behavior. The region where the concentration approaches the maximum value is associated with the bed layer. The upper region corresponds to the suspended particles region (the heterogeneous layer).

The dimensionless local heat transfer coefficient changes from its lowest value, below unity at the bottom of the pipe, to values above unity at the upper heterogeneous layer. For the case of $Re_w = 55\ 000$ the local heat transfer coefficient in contact with the bed layer is about 10–

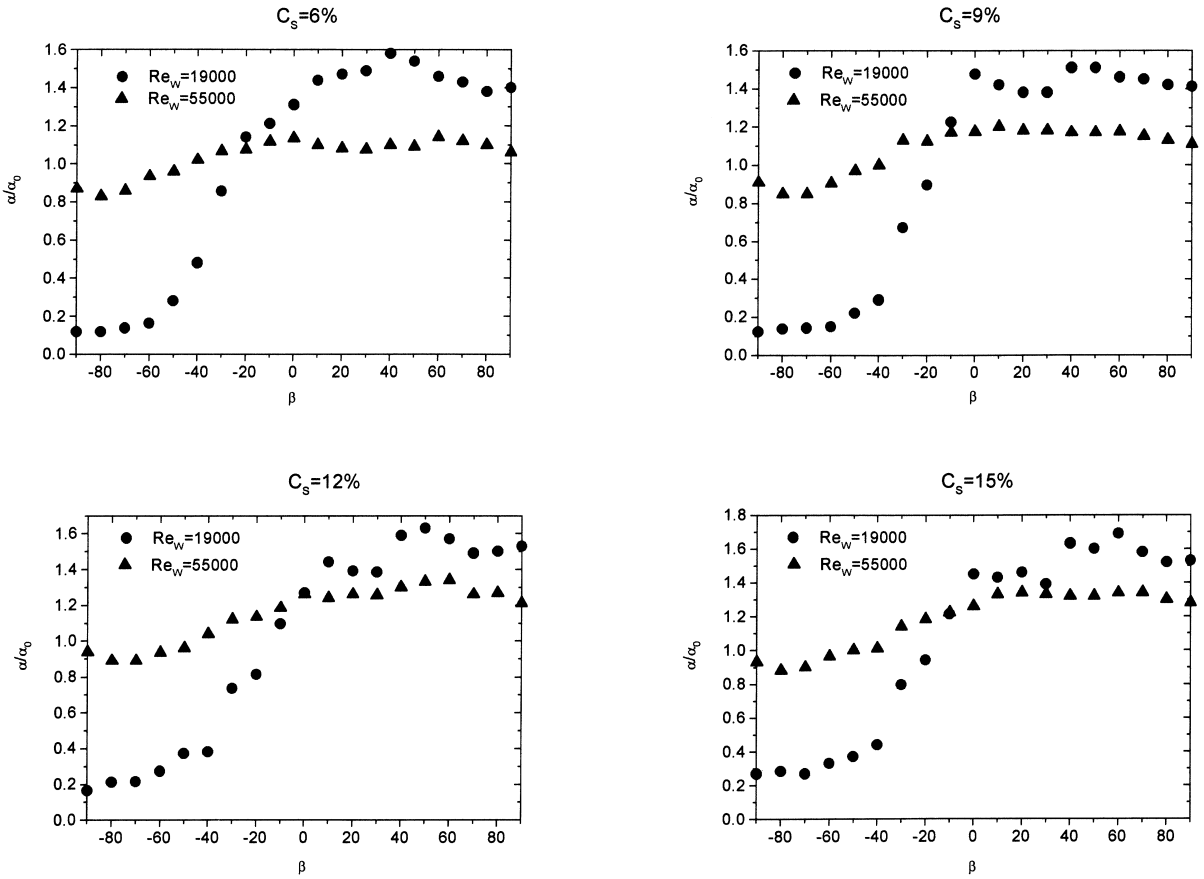

Fig. 5. Local heat transfer coefficient — comparison between $Re_W = 19\ 000$ and $Re_W = 55\ 000$.

15% lower than that in clear liquid, while, at the upper part it is up to 35% above the value in clear water (Fig. 3). Near the upper wall the heat transfer coefficients approach the value of clear liquid. For the case of $Re_w = 19\,000$ (Fig. 4) the average bed thickness is greater than the one observed for $Re_w = 55\,000$ and it is more compact (see concentration profiles). As a result the variation of the local heat transfer coefficient has a much wider range. At the bottom of the pipe the heat transfer coefficient is about 8-fold lower than for clear water due to the insulating effect of the packed bed. On the other hand an increase of about 60% can be observed in the upper heterogeneous region. This is attributed to the smaller gap of the heterogeneous layer in this case. A comparison between the two regimes ($Re_w = 19\,000$ and 55 000) is shown in Fig. 5 where the local heat transfer coefficient is plotted as a function of the angular coordinate. One can notice the drastic decrease of the dimensionless heat transfer

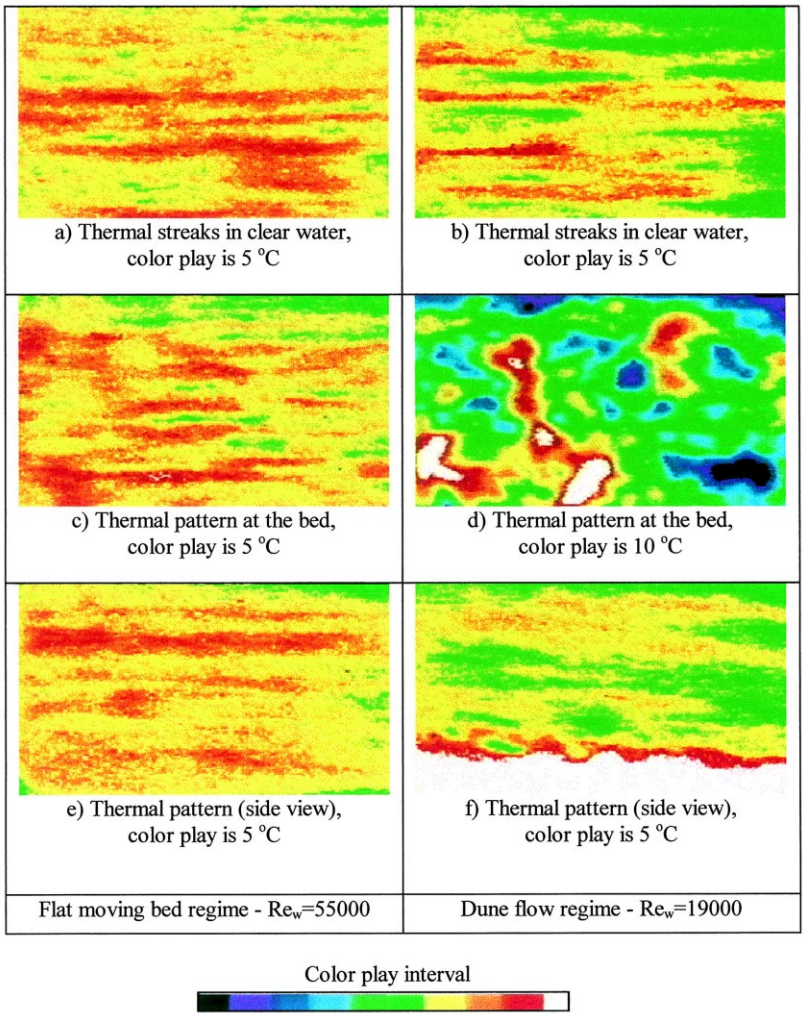

Fig. 6. Temperature fields.

coefficient in the bed layer corresponding to relatively low mixture velocities ($Re_w = 19\,000$, the dune regime), compared with a relatively "smooth" variation of the heat transfer coefficient associated with high mixture velocities ($Re_w = 55\,000$, the flat bed regime).

Fig. 6 illustrates the wall temperature fields as obtained by the IR camera. Each image presents an window of 70° opening. The images in 6(c) and 6(e) exhibit the near wall structure corresponding to the flat bed regime ($Re_w = 55\,000$). From the images it can be observed that this streaky structure is similar to the one observed in clear liquid flow [Fig. 6(a)]. All images were obtained at the same heat flux.

The structure near the wall changes drastically for the case of $Re_w = 19\,000$ (the dune flow regime). The streaky structure typical to clear water flow [Fig. 6(b)] is completely destroyed in the bed [Fig. 6(d)]. We had to decrease the heat flux by a factor of four, simultaneously

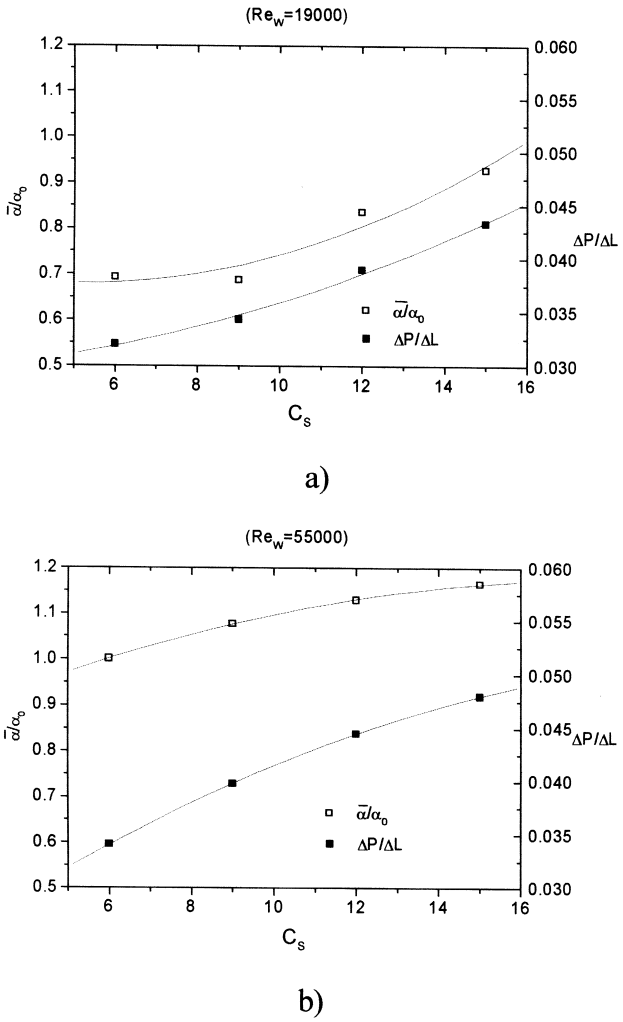

Fig. 7. Average heat transfer coefficient and pressure drop vs delivery concentration.

doubling the color play interval, to observe the changes in the thermal patterns. The "overheated" zone can easily be noticed at the bottom (side view) of the thermal field in the dune regime [Fig. 6(f)]. Nevertheless, above the bed region the thermal streaks can be observed.

The effect of the delivery concentration, C_S, on the cross sectional average heat transfer coefficient and on the pressure drop is shown in Fig. 7. As can be seen these too parameters increase with the delivery concentration for the dune regime as well as for the flat bed regime. At low mixture velocities [Fig. 7(a)] the average heat transfer coefficient is lower than the one for clear water (at the same Reynolds number), while for high mixture flow rates the average heat transfer coefficient is higher [Fig. 7(b)].

The concentration profiles (Figs. 3 and 4) were fitted using a modified Boltzman function of the form

$$C = \frac{C_{\max}}{1 + \exp\left(\dfrac{\bar{h} - \bar{h}_0}{\Delta\bar{h}}\right)} \tag{5}$$

where $C_{\max}$ is the bed concentration, $\bar{h} = h/D$ the dimensionless height, $\bar{h}_0$ the moving bed average height and $\Delta\bar{h}$ a term representing the profile slope at $\bar{h}_0$. $C_{\max}$ is assumed to be 0.52 (cubic packing for spheres). The best fit is obtained for Δh given by the following linear relation,

$$\Delta h = 0.22 + 0.0164 C_s \tag{6}$$

and for $\bar{h}_0$ given in Fig. 8.

The values of $\bar{h}_0$ are compared in Fig. 8 to the bed height obtained by the three-layer model (Doron and Barnea, 1993).

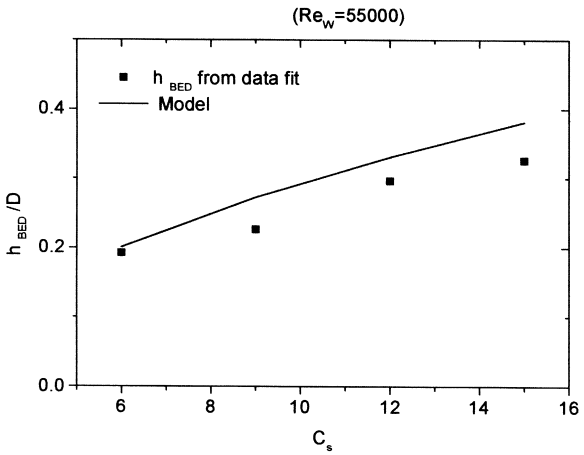

Fig. 8. Bed height — experimental data and the three-layer model prediction.

4. Conclusions

An experimental study of the heat transfer, associated with solid–liquid mixture transport was carried out by using an electro-resistance sensor and infrared imaging. The local value of the heat transfer coefficient is strongly influenced by the distribution of the solid phase in the pipe cross section. At flow regimes associated with low mixture flow rates and substantial settled bed the heat transfer at the bed periphery deteriorates because of the "insulating effect" produced by the settled particles. In some cases, this phenomenon may cause local overheating. The heat transfer increase above the bed can be explained by the increase of the average mixture velocity in the upper region of the pipe and by the mixing effect of the particles.

The near wall structure, as inferred from the temperature field, has shown that at velocities associated with the flat moving bed regime, the streaky structure is close to the one observed in clear liquid.

It is shown that the modified Boltzman function fits the concentration profiles both for the dune and the flat bed regimes. Good agreement is observed between the bed height available from experimental data, and the one predicted by the three-layer model.

Acknowledgements

This research was supported by the Fund for the Promotion of Research at the Technion. Dr R. Rozenblit is partially supported by the Center for Absorption in Science, Ministry of Immigrants Absorption, State of Israel.

References

Agarwal, P.K., 1988. Transport phenomena in multi-particles systems–II. Particle–fluid heat and mass transfer. Chem. Eng. Sci. 43, 2501–2510.

Creutz, M., Mewes, D., 1999. A novel centrifugal gas-liquid separator for catching intermittent flows, Int. J. Multiphase Flow. (In press).

Doron, P., Barnea, D., 1993. A three layer model for solid liquid flow in horizontal pipes. Int. J. Multiphase Flow 19, 1029–1043.

Doron, P., Barnea, D., 1996. Flow pattern maps for solid liquid flow in pipes. Int. J. Multiphase Flow 22, 273–283.

Foster, J., Nasr-el-Din, H.A., Masliyah, J.H., 1992. Solids distribution in slurry flow in a linear manifold with a horizontal approach. Can. J. Chem. Eng. 70, 3–12.

Harada, E., Kuriyama, M., Konno, H., 1989. Heat transfer with a solid liquid suspension flowing through a horizontal rectangular duct. Heat Transfer — Japanese Research 18, 79–94.

Harada, E., Toda, M., Kuriyama, M., Konno, H., 1985. Heat transfer between wall and solid-water suspension flow in horizontal pipes. J. Chem. Eng. Japan 18, 33–38.

Hasegawa, S., Echido, R., Kanemaru, K., Ichimiya, K., Samui, M., 1983. Experimental study of forced convective heat transfer of flowing gaseous solid suspensions at high temperature. Int. J. Multiphase Flow 9, 131–145.

Hetsroni, G., Rozenblit, R., 1994. Heat transfer to a solid–liquid mixture in a flume. Int. J. Multiphase Flow 20, 671–689.

Hetsroni, G., Hu, B.G., Yi, J.H., Mosyak, A., Yarin, L.P., Ziskind, G., 1998. Heat transfer in intermittent air-water flows. Part I — Horizontal tube. Int. J. Multiphase Flow 24, 165–188.

Kaftori, D., Hetsroni, G., Banerjee, S., 1995. Particle behavior in the turbulent boundary layer. I-Motion, deposition and entrainment. Phys. Fluids 7, 1095–1106.

Nasr-el-din, H., Shook, C.A., Colwell, J., 1987. A conductivity probe for measuring local concentrations in slurry systems. Int. J. Multiphase Flow 13, 365–378.

Nino, Y., Garsia, M.H., 1996. Experiments on particle-turbulence interactions in the near-wall region of the open channel flow: implication for sediment transport. J. Fluid Mech. 326, 285–319.

Quader, A.K.M.A., Wilkinson, W.L., 1981. Turbulent heat transfer to dilute aqueous suspensions of titanium dioxide in pipes. Int. J. Multiphase Flow 7, 545–554.

Ozbelge, T.A., Somer, T.G., 1988. Hydrodynamic and heat transfer characteristics of solid–liquid suspensions in horizontal turbulent pipe flow. Chem. Eng. J. 38, 111–122.

Simkhis, M., Barnea, D., Taitel, Y., 1998. Hydrodynamic characteristics of wave like flow in solid–liquid mixtures in pipes. Third Int. Conf. on Multiphase flow, Lyon, France.

Shook, C.A., Roco, M.C., 1991. Slurry Flow: Principles and Practice. Butterworth–Heinemann, Boston.

Thomas, G.D., 1964. Transport characteristics of suspensions. Part IX. Transport phenomena on a flow regime diagram for dilute suspension transport. A.I.Ch.E. J. 10 (3), 303–308.

Taylor, G., 1954. The dispersion of matter in turbulent flow through a pipe. Proc. Roy. Soc. Lond. A223, 446–468.

Televantos, Y., Shook, C.A., Carleton, A., Street, M., 1979. Flow of slurries of coarse particles at high solid concentration. Can. J. Chem. Eng. 57, 255–262.

Wilkinson, G.T., Norman, J.R., 1967. Heat transfer to a suspension of solids in a gas. Trans. Int. Chem. Eng. 45, 314–318.

Wilson, K.C., Street, M., Bantin, R.A., 1972. Slip model correlation of dense two phase flow. Proc. 2nd Int. Conf. on Hydraulic Transport of Solids in Pipes, BHRA, Cranfield, UK, Paper B1.